The Canadian Mineralogist
Vol. 39, pp. 1161-1170 (2001)

Li-BEARING ARFVEDSONITIC AMPHIBOLES FROM THE STRANGE LAKE PERALKALINE GRANITE, QUEBEC

FRANK C. HAWTHORNE[§], ROBERTA OBERTI, ELIO CANNILLO AND LUISA OTTOLINI

CNR Centro di Studio per la Cristallochimica e la Cristallografia, via Ferrata 1, I–27100 Pavia, Italy

JEANETTE N. ROELOFSEN AND ROBERT F. MARTIN

Department of Earth and Planetary Sciences, McGill University, Montreal, Quebec H3A 2A7, Canada

ABSTRACT

The crystal structures of seven sodic amphiboles from the Strange Lake peralkaline granite, on the Quebec–Labrador border, have been refined to *R* values of 1.3–1.7% using single-crystal Mo*K*α X-ray data. Crystals used in the collection of the intensity data were subsequently analyzed by electron- and ion-microprobe methods. Site occupancies were assigned by site-scattering refinement and stereochemical considerations, taking into account the electron- and ion-microprobe data for each crystal. These amphiboles are lithian arfvedsonite and lithian manganoan arfvedsonite, and have anomalously low X-ray scattering at the *M*(3) site. Ion-microprobe analysis shows the presence of significant Li in all of these samples (up to 0.63 wt%, equivalent to 0.40 Li *apfu*), and the site-scattering refinement shows Li to be completely ordered at the *M*(3) site. Ion-microprobe analysis also shows evidence of limited dehydrogenation that correlates with the amount of Ti in the amphibole. The amphiboles show several interesting chemical correlations: (1) the Mn and Zn contents show a very strong positive correlation; (2) the K and Al contents ($0.02 < Al < 0.08$ *apfu* are inversely correlated; (3) the Li and Ca contents show a strong negative correlation. The sample order in correlations (1) and (2) is the same, supporting the idea that these correlations are petrogenetic rather than crystal-chemical. Moreover, similar correlations occur in similar amphiboles from the Virgin Canyon pluton, New Mexico.

Keywords: amphibole, arfvedsonite, crystal-structure refinement, electron-microprobe analysis, ion-microprobe analysis, H content, Li content, peralkaline granite, Strange Lake, Quebec–Labrador.

SOMMAIRE

Nous avons affiné la structure cristalline de sept échantillons d'amphibole sodique provenant du granite hyperalcalin de Strange Lake, sur la frontière Québec–Labrador, jusqu'à un résidu dans l'intervalle 1.3–1.7% en utilisant des données en diffraction X sur cristaux uniques, prélevées avec rayonnement Mo*K*α. Les cristaux utilisés ont ensuite été analysés par microsondes électronique et ionique. L'occupation des sites a été assignée par affinement de la dispersion associée aux divers sites et selon des considérations stéréochimiques, en tenant compte des données obtenues sur la composition de chaque cristal. Sont représentés l'arfvedsonite lithinifère et l'arfvedsonite lithinifère manganifère. Les sept échantillons contiennent des teneurs importantes en Li (jusqu'à 0.63%, en poids, l'équivalent de 0.40 Li atomes par unité formulaire, *apuf*), et les affinements de la dispersion aux sites montrent que le Li est complètement ordonné au site *M*(3). Les données obtenues avec la microsonde ionique indiquent aussi un déficit en hydrogène lié à la teneur en titane de l'amphibole. Les échantillons d'amphibole montrent plusieurs corrélations intéressantes: (1) les teneurs en Mn et en Zn montrent une corrélation positive marquée; (2) les teneurs en K et en Al ($0.02 < Al < 0.08$ *apuf*) montrent un corrélation inverse; (3) les teneurs en Li et en Ca montrent une corrélation négative. La séquence des échantillons des corrélations (1) et (2) sont les mêmes, ce qui fait penser qu'elles seraient plutôt d'origine pétrogénétique que cristallochimique. De plus, des corrélations semblables ont été documentées pour des amphiboles semblables dans le pluton de Virgin Canyon, au Nouveau-Mexique.

(Traduit par la Rédaction)

Mots-clés: amphibole, arfvedsonite, affinement de la structure cristalline, données de microsonde électronique, données de microsonde ionique, teneur en H, teneur en Li, granite hyperalcalin, Strange Lake, Québec–Labrador.

§ Usually imprisoned at: Department of Geological Sciences, University of Manitoba, Winnipeg, Manitoba R3T 2N2, Canada. *E-mail address*: frank_hawthorne@umanitoba.ca

INTRODUCTION

Sodic amphiboles occur in a wide variety of geological environments, but are particularly characteristic of peralkaline (agpaitic) igneous rocks and their metamorphosed equivalents. In such peralkaline igneous rocks, which crystallize from geochemically evolved magmas, the sodic amphibole hosts elements not normally encountered in rock-forming amphiboles (*e.g.*, Li). Hawthorne *et al.* (1992, 1993, 1994, 1996a, b, 1998) have characterized the role of Li in sodic amphiboles, and have shown how recognition of the presence of Li leads to improved estimation of the oxidation ratio of iron, and ultimately to correct structural formulae. Three Li-bearing sodic amphiboles have been recognized recently: leakeite, $Na\ Na_2\ (Mg_2Fe^{3+}{}_2Li)\ Si_8\ O_{22}\ (OH)_2$ (Hawthorne *et al.* 1992), kornite, $K\ Na_2\ (Mg_2Mn^{3+}{}_2Li)\ Si_8\ O_{22}\ (OH)_2$ (Armbruster *et al.* 1993) and fluoroferroleakeite (Hawthorne *et al.* 1996a).

Lithium is expected to be an important constituent of sodic amphibole in the Strange Lake peralkaline granite pluton, located near Lac Brisson, astride the Quebec–Labrador border about 250 km north of Schefferville, Quebec. This small granite pluton (8 km across) is mineralized; an unusual assemblage of secondary minerals of Zr, Nb, rare-earth elements and Li occurs in altered variants of the most evolved intrusive unit, near the core of the pluton. Lithium-bearing arfvedsonitic amphibole is present from the least evolved to the most evolved members of the Strange Lake suite. We focus here on the structure and crystal chemistry of a suite of sodic amphibole that is relatively enriched in Li, Zn, Zr, Mn and K, and depleted in Mg, Ca and Al.

GEOLOGICAL CONTEXT

We chose seven representative samples (Table 1). The Strange Lake magma was already geochemically evolved when it was emplaced in the middle crust during the Middle Proterozoic. The most primitive granite exposed is a Mg-depleted low-Ca hypersolvus granite cut by sparse pegmatite dikes; these rocks show only minimal signs of a hydrothermal overprint. With massive crystallization of anhydrous minerals (quartz, alkali feldspar), the magma reached saturation in an aqueous fluid phase, and a subsolvus assemblage of two magmatic feldspars (albite + K-feldspar, now microcline) appeared. Fresh samples of the subsolvus granite are available, but as one approaches the center of the pluton, hydrothermally affected subsolvus granite is the norm. In the ore zone, layered pegmatite–aplite sills and their altered subsolvus-facies host-rocks are highly enriched in an assemblage of potential ore constituents: gittinsite, kainosite-(Y), gerenite-(Y), gadolinite-(Y), narsarsukite, armstrongite, elpidite, yttrian milarite and Li-bearing mica (Birkett *et al.* 1992, Miller 1996, Roelofsen 1997, and references therein). Boily & Williams-Jones (1994) described the roles of magmatic and hydrothermal processes in the evolution of the Strange Lake complex. Our sampling includes an unusual mafic lens of flow-oriented fine-grained prisms of arfvedsonite crystallized in the pegmatite–aplite sills of the ore zone from a highly evolved and alkaline derivative magma of mafic character.

TABLE 1. SAMPLE NUMBERS FOR STRANGE LAKE AMPHIBOLES

This work	Occurrence	Original	*Seq.
SL(1)	Ore zone, coarse-grained	SL–1–17	654
SL(2)	Mafic region, fine-grained	BS	655
SL(3)	Hypersolvus, pegmatitic	48–A–7	656
SL(4)	Subsolvus granite	54–A–1	658
SL(5)	Hypersolvus granite	49–C–2	660
SL(6)	Hypersolvus granite	46–I–3	661
SL(7)	Subsolvus granite	63–B–3	663

* Sequence number in CNR-CSCC amphibole database.

EXPERIMENTAL

X-ray data collection and structure refinement

Experimental details are as described by Oberti *et al.* (1992). Unit-cell data, *R* values and other information pertinent to intensity-data collection and structure refinement are given in Table 2. Final atom coordinates and displacement parameters are listed in Table 3. Observed and calculated structure-factors are available from The Depository of Unpublished Data, CISTI, National Research Council, Ottawa, Ontario K1A 0S2, Canada. Selected interatomic distances and angles are given in Table 4, and refined site-scattering values are listed in Table 5.

Electron-microprobe analysis

Subsequent to the collection of the X-ray intensity data, the crystals were mounted in epoxy, polished and analyzed by electron- and ion-microprobe techniques (the latter for H, Li and F) following the procedures

TABLE 2. CELL DIMENSIONS* AND STRUCTURE-REFINEMENT INFORMATION FOR STRANGE LAKE AMPHIBOLES

	SL(1)	SL(2)	SL(3)	SL(4)	SL(5)	SL(6)	SL(7)
a (Å)	9.876	9.913	9.875	9.861	9.874	9.912	9.893
b	18.036	18.029	18.026	18.033	18.054	18.050	18.044
c	5.315	5.315	5.314	5.318	5.318	5.314	5.315
β (°)	103.74	103.75	103.71	103.68	103.66	103.77	103.68
V (Å^3)	919.6	922.7	919.0	918.8	921.2	923.4	921.9
No. *I*	1390	1397	1387	1394	1394	1398	1392
No. $\|F_o\|$	1018	951	1049	981	1112	1099	1037
R(obs)	1.37	1.39	1.4	1.47	1.68	1.68	1.44
R(all)	2.82	3.62	2.59	3.39	2.56	2.63	2.74

* Standard deviations are ≤2 in the last significant figure.

TABLE 3. ATOM PARAMETERS AND DISPLACEMENT FACTORS FOR STRANGE LAKE AMPHIBOLES

	x	y	z	β_{11}	β_{22}	β_{33}	β_{12}	β_{13}	β_{23}
SL(1)									
O(1)	0.11136	0.09083	0.20892	0.0017	0.001	0.0066	−0.0001	0.001	−0.0002
O(2)	0.12029	0.17135	0.7334	0.0018	0.001	0.0077	0	0.001	−0.0001
O(3)	0.11203	0	0.70634	0.0037	0.001	0.0117	0	0.0014	0
O(4)	0.36432	0.24814	0.80034	0.0037	0.001	0.0088	−0.0005	0.0021	−0.0004
O(5)	0.34784	0.1267	0.07866	0.0018	0.001	0.0072	0	0.0011	0
O(6)	0.34093	0.11958	0.57779	0.0021	0.001	0.0063	0	0.001	−0.0007
O(7)	0.33239	0	0.29803	0.0032	0	0.0127	0	0.0013	0
T(1)	0.27831	0.08571	0.29027	0.0015	0	0.0046	0	0.001	0
T(2)	0.28882	0.17027	0.79929	0.0014	0	0.0045	−0.0001	0.001	0
M(1)	0	0.08981	1/2	0.0021	0.001	0.0058	0	0.0011	0
M(2)	0	0.18265	0	0.0014	0	0.0055	0	0.001	0
M(3)	0	0	0	0.0022	0	0.0059	0	0	0
M(4)	0	0.27698	1/2	0.0041	0.001	0.0171	0	0.0054	0
A	0	1/2	0	0.0031	0.0012	0.019	0	0.001	0
A(*m*)	0.05009	1/2	0.10446	0.0101	0.0016	0.0309	0	0.0118	0
SL(2)									
O(1)	0.11042	0.09164	0.20832	0.0014	0.001	0.0054	−0.0001	0	0
O(2)	0.12023	0.1723	0.73461	0.0019	0.001	0.0066	0	0.001	−0.0002
O(3)	0.11176	0	0.70622	0.0031	0.001	0.0109	0	0.001	0
O(4)	0.36463	0.24802	0.80054	0.0035	0.001	0.0072	−0.0005	0.0023	−0.0004
O(5)	0.3465	0.12652	0.07888	0.0018	0.001	0.006	−0.0001	0.0012	0
O(6)	0.33905	0.11983	0.57834	0.002	0.001	0.0055	0	0.001	−0.0007
O(7)	0.32908	0	0.30039	0.0029	0	0.013	0	0.002	0
T(1)	0.27612	0.08599	0.2902	0.0015	0	0.0037	0	0.001	0
T(2)	0.28785	0.17066	0.79982	0.0014	0	0.0038	−0.0001	0.001	−0.0001
M(1)	0	0.09016	1/2	0.002	0.001	0.0053	0	0.0013	0
M(2)	0	0.18305	0	0.0014	0	0.0047	0	0.001	0
M(3)	0	0	0	0.0023	0	0.0056	0	0	0
M(4)	0	0.27751	1/2	0.0041	0.001	0.0154	0	0.005	0
A	0	1/2	0	0.0073	0.0013	0.0274	0	0.0141	0
A(*m*)	0.04753	1/2	0.10121	0.0105	0.0012	0.0309	0	0.013	0
H	0.17094	0	0.73785	1.3863	0	0	0	0	0
SL(3)									
O(1)	0.11148	0.08979	0.20751	0.0015	0.001	0.0054	−0.0001	0.001	−0.0002
O(2)	0.12041	0.17158	0.73307	0.002	0.001	0.0069	0	0.001	−0.0002
O(3)	0.11148	0	0.70751	0.0038	0.001	0.0103	0	0.0023	0
O(4)	0.3641	0.24839	0.79869	0.0037	0.001	0.0085	−0.0004	0.0024	−0.0003
O(5)	0.34794	0.12687	0.07731	0.0018	0.001	0.0067	0	0.0012	0
O(6)	0.34054	0.11942	0.57683	0.0023	0.001	0.0056	0	0.001	−0.0008
O(7)	0.33393	0	0.29714	0.0026	0	0.0131	0	0.0016	0
T(1)	0.27859	0.08555	0.289	0.0015	0	0.0039	0	0.001	0
T(2)	0.28881	0.17044	0.79837	0.0014	0	0.0037	−0.0002	0.001	−0.0001
M(1)	0	0.09078	1/2	0.0021	0.001	0.0051	0	0.0013	0
M(2)	0	0.18278	0	0.0014	0	0.005	0	0.001	0
M(3)	0	0	0	0.002	0	0.0049	0	0.001	0
M(4)	0	0.27665	1/2	0.004	0.001	0.0161	0	0.0053	0
A	0	1/2	0	0.0063	0.0014	0.0351	0	0.0147	0
A(*m*)	0.0518	1/2	0.10947	0.0105	0.002	0.0303	0	0.0121	0
SL(4)									
O(1)	0.11158	0.09043	0.20821	0.0014	0.001	0.0054	−0.0001	0.001	−0.0002
O(2)	0.12042	0.17151	0.73441	0.0018	0.001	0.0067	0	0.001	−0.0002
O(3)	0.11193	0	0.70589	0.0037	0.001	0.0111	0	0.0015	0
O(4)	0.36462	0.24834	0.79919	0.0036	0.001	0.0078	−0.0004	0.002	−0.0001
O(5)	0.34847	0.12689	0.07831	0.0018	0.001	0.0063	−0.0001	0.0011	0
O(6)	0.34103	0.11961	0.57735	0.0022	0.001	0.0057	0	0.001	−0.0007
O(7)	0.33385	0	0.29707	0.003	0	0.013	0	0.0012	0
T(1)	0.27883	0.08563	0.28957	0.0015	0	0.0038	0	0.001	0
T(2)	0.28915	0.17043	0.79913	0.0015	0	0.0038	−0.0001	0.001	−0.0001
SL(4) (continued)									
M(1)	0	0.09075	1/2	0.002	0.001	0.0053	0	0.0011	0
M(2)	0	0.18273	0	0.0014	0	0.005	0	0.001	0
M(3)	0	0	0	0.0022	0	0.005	0	0.001	0
M(4)	0	0.27686	1/2	0.0039	0.001	0.0158	0	0.0049	0
A	0	1/2	0	0.0037	0.0016	0.025	0	0.0096	0
A(*m*)	0.0517	1/2	0.10869	0.0097	0.0017	0.0282	0	0.011	0
SL(5)									
O(1)	0.1117	0.09013	0.20773	0.0015	0.001	0.0052	−0.0001	0.001	−0.0001
O(2)	0.12069	0.1714	0.73242	0.0018	0.001	0.0063	0	0	−0.0001
O(3)	0.11198	0	0.70596	0.0038	0.001	0.0096	0	0.0018	0
O(4)	0.36392	0.24826	0.79958	0.0035	0.001	0.0078	−0.0005	0.002	−0.0003
O(5)	0.34821	0.12672	0.07759	0.0019	0.001	0.0064	0	0.001	0
O(6)	0.34098	0.11947	0.57725	0.0023	0.001	0.0056	0	0.001	−0.0007
O(7)	0.33358	0	0.29722	0.0029	0	0.0121	0	0.0017	0
T(1)	0.27882	0.08559	0.28934	0.0014	0	0.0036	0	0.001	0
T(2)	0.28886	0.17031	0.79853	0.0014	0	0.0036	−0.0001	0.001	0
M(1)	0	0.09066	1/2	0.0019	0.001	0.0048	0	0.0011	0
M(2)	0	0.18292	0	0.0014	0	0.0049	0	0.001	0
M(3)	0	0	0	0.002	0	0.0044	0	0	0
M(4)	0	0.27682	1/2	0.0043	0.001	0.0156	0	0.0054	0
A	0	1/2	0	0.0042	0.0017	0.0214	0	0.0095	0
A(*m*)	0.05287	1/2	0.10954	0.0103	0.0019	0.029	0	0.0117	0
SL(6)									
O(1)	0.11109	0.09053	0.20888	0.0015	0.001	0.0064	−0.0001	0.001	−0.0001
O(2)	0.12014	0.17155	0.73286	0.0016	0.001	0.0073	0	0	0
O(3)	0.11146	0	0.70742	0.0034	0.001	0.0113	0	0.0013	0
O(4)	0.36381	0.24793	0.79967	0.0035	0.001	0.0086	−0.0006	0.0019	−0.0003
O(5)	0.34689	0.12658	0.07824	0.0018	0.001	0.0062	0	0.001	0
O(6)	0.34022	0.11936	0.57828	0.0021	0.001	0.0055	0	0.001	−0.0007
O(7)	0.33132	0	0.29859	0.0028	0	0.0126	0	0.001	0
T(1)	0.2774	0.08571	0.2901	0.0014	0	0.0043	−0.0001	0	0
T(2)	0.28802	0.17048	0.79882	0.0013	0	0.0044	−0.0001	0.001	−0.0001
M(1)	0	0.09014	1/2	0.0019	0.001	0.0059	0	0.0011	0
M(2)	0	0.18298	0	0.0013	0	0.0056	0	0.001	0
M(3)	0	0	0	0.002	0	0.0058	0	0	0
M(4)	0	0.27704	1/2	0.0039	0.001	0.0176	0	0.0049	0
A	0	1/2	0	0.0053	0.001	0.0246	0	0.0114	0
A(*m*)	0.04718	1/2	0.10094	0.0094	0.0015	0.0294	0	0.0113	0
SL(7)									
O(1)	0.11103	0.09098	0.20827	0.0018	0.001	0.0059	−0.0001	0.001	−0.0002
O(2)	0.1204	0.17191	0.73387	0.0019	0.001	0.0069	0	0.001	−0.0001
O(3)	0.11224	0	0.70664	0.0038	0.001	0.0104	0	0.0018	0
O(4)	0.36462	0.24808	0.80005	0.0038	0.001	0.0082	−0.0005	0.0022	−0.0003
O(5)	0.34742	0.12688	0.07893	0.0022	0.001	0.0061	0	0.0013	0
O(6)	0.34009	0.11941	0.57808	0.0024	0.001	0.0053	0	0.001	−0.0007
O(7)	0.33087	0	0.29818	0.0027	0	0.0131	0	0.0014	0
T(1)	0.27753	0.08578	0.29004	0.0016	0	0.004	0	0.001	0
T(2)	0.28853	0.17049	0.79951	0.0015	0	0.004	−0.0001	0.001	−0.0001
M(1)	0	0.09048	1/2	0.0022	0.001	0.0053	0	0.0014	0
M(2)	0	0.18293	0	0.0016	0	0.005	0	0.001	0
M(3)	0	0	0	0.0024	0	0.0054	0	0.001	0
M(4)	0	0.27727	1/2	0.0043	0.001	0.0156	0	0.0054	0
A	0	1/2	0	0.0046	0.0012	0.0208	0	0.0097	0
A(*m*)	0.04861	1/2	0.10259	0.0096	0.0014	0.0309	0	0.0123	0

TABLE 4. SELECTED INTERATOMIC DISTANCES (Å) AND ANGLES (°) IN STRANGE LAKE AMPHIBOLES*

	SL(1)	SL(2)	SL(3)	SL(4)	SL(5)	SL(6)	SL(7)
T(1)–O(1)	1.605	1.599	1.605	1.605	1.606	1.604	1.604
T(1)–O(5)	1.628	1.629	1.629	1.629	1.629	1.629	1.629
T(1)–O(6)	1.625	1.627	1.626	1.628	1.628	1.627	1.627
T(1)–O(7)	1.633	1.634	1.633	1.634	1.634	1.634	1.632
<*T*(1)–O>	1.623	1.622	1.623	1.624	1.624	1.624	1.623
T(2)–O(2)	1.618	1.615	1.616	1.618	1.614	1.617	1.617
T(2)–O(4)	1.589	1.588	1.590	1.590	1.590	1.587	1.589
T(2)–O(5)	1.66	1.662	1.657	1.659	1.660	1.661	1.660
T(2)–O(6)	1.666	1.665	1.667	1.67	1.667	1.668	1.667
<*T*(2)–O>	1.633	1.633	1.632	1.633	1.633	1.633	1.633
M(1)–O(1) x2	2.100	2.100	2.107	2.104	2.108	2.102	2.101
M(1)–O(2) x2	2.100	2.112	2.091	2.094	2.092	2.099	2.103
M(1)–O(3) x2	2.115	2.120	2.128	2.127	2.128	2.122	2.128
<*M*(1)–O>	2.105	2.111	2.109	2.108	2.109	2.108	2.111
M(2)–O(1) x2	2.146	2.136	2.159	2.152	2.161	2.156	2.147
M(2)–O(2) x2	2.064	2.061	2.066	2.059	2.071	2.069	2.063
M(2)–O(4) x2	1.950	1.948	1.950	1.948	1.951	1.956	1.949
<*M*(2)–O>	2.053	2.048	2.058	2.053	2.061	2.060	2.053
M(3)–O(1) x4	2.132	2.139	2.115	2.126	2.123	2.129	2.133
M(3)–O(3) x2	2.117	2.118	2.107	2.117	2.118	2.111	2.117
<*M*(3)–O>	2.127	2.132	2.112	2.123	2.121	2.123	2.128
M(4)–O(2) x2	2.43	2.422	2.416	2.423	2.424	2.423	2.424
M(4)–O(4) x2	2.359	2.363	2.352	2.350	2.358	2.363	2.357
M(4)–O(5) x2	2.948	2.950	2.954	2.948	2.955	2.955	2.946
M(4)–O(6) x2	2.535	2.544	2.542	2.533	2.539	2.548	2.542
<*M*(4)–O>	2.567	2.570	2.566	2.564	2.569	2.572	2.567
A–O(5) x4	2.820	2.828	2.819	2.817	2.818	2.828	2.828
A–O(6) x4	3.237	3.243	3.239	3.240	3.241	3.238	3.240
A–O(7) x2	2.548	2.589	2.532	2.531	2.535	2.565	2.562
<*A*–O>	2.933	2.946	2.930	2.929	2.931	2.939	2.939
A(*m*)–O(5)	2.766	2.775	2.768	2.767	2.764	2.776	2.775
A(*m*)–O(5)	3.017	3.013	3.025	3.021	3.031	3.010	3.017
A(*m*)–O(6)	2.792	2.812	2.775	2.779	2.775	2.808	2.802
A(*m*)–O(7)	2.595	2.627	2.577	2.576	2.590	2.598	2.604
A(*m*)–O(7)	2.665	2.700	2.664	2.661	2.661	2.679	2.676
A(*m*)–O(7)	3.111	3.124	3.087	3.094	3.088	3.131	3.125
A–*A*(*m*)	0.650	0.625	0.678	0.674	0.684	0.622	0.636
T(1)–O(5)–*T*(2)	135.8	135.5	135.9	135.8	135.8	135.8	135.7
T(1)–O(6)–*T*(2)	139.3	139.3	139.6	139.6	139.5	139.0	139.4
T(1)–O(7)–*T*(1)	142.4	143.2	141.5	141.8	142.0	142.5	142.9

* Standard deviations are 1 or less in the final figure.

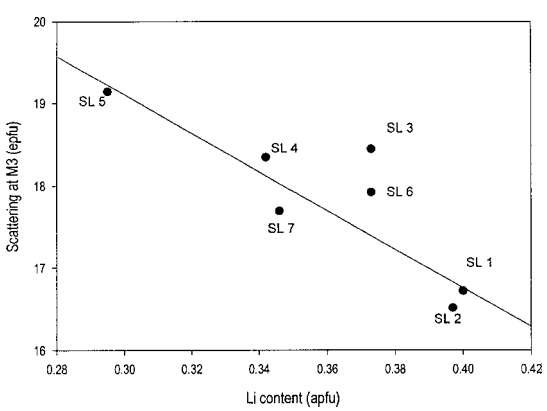

FIG. 1. Variation in the refined site-scattering at the *M*(3) site as a function of Li content of the amphibole; the line is the ideal relation for all Li to substitute for Fe at the *M*(3) site.

described by Oberti *et al.* (1992) and Ottolini *et al.* (1993, 1995). Chemical compositions (Table 6) are the mean of at least 10 determinations on the same crystal, and hence should be representative of the bulk composition of the crystal, particularly as no significant compositional zoning was detected in any of the crystals. The Fe^{3+}/Fe^{2+} values were derived as described by Hawthorne *et al.* (1993), taking into account the presence of partial dehydrogenation. Unit formulae were calculated on the basis of 24(O,OH,F); the agreement between the refined site-scattering values and analogous values calculated from the unit formulae (Table 6) is very close (±1%). Sample SL(2) is a lithian manganoan arfvedsonite; the rest of the samples are lithian arfvedsonite.

DISCUSSION

The general details of the arfvedsonite structure were described by Kawahara (1963) and Hawthorne (1978, 1983), and the crystal-chemical aspects of Li incorporation into eckermannite and arfvedsonite were discussed by Hawthorne *et al.* (1993, 1994). Inspection of the <*T*–O> distances (Table 4) indicates that all $^{[4]}$Al is ordered at the *T*(1) site (Hawthorne 1983, Oberti *et al.* 1995).

The behavior of Li

From previous work, we expect Li to be a *C*-group cation and to be completely ordered at the *M*(3) site; the observed site-scattering values (Table 5) indicate this to be the case. Figure 1 shows the refined site-scattering at the *M*(3) site as a function of the Li content of the amphibole. The observed values scatter about the ideal line for Li ⇌ Fe substitution, in accord with ordering of Li at the *M*(3) site in these amphiboles. We can express this relation more directly by plotting the relative scattering at *M*(1) *versus* *M*(3) against the Li content (as measured by ion-microprobe analysis) in all structures

TABLE 5. REFINED SITE-SCATTERING VALUES (*epfu*) FOR STRANGE LAKE AMPHIBOLES

	SL(1)	SL(2)	SL(3)	SL(4)	SL(5)	SL(6)	SL(7)
M(1)	51.09	51.67	51.81	51.87	51.49	51.64	51.65
M(2)	51.81	51.79	51.65	51.62	51.85	52.46	51.76
M(3)	16.72	16.51	18.44	18.34	19.14	17.92	17.69
Σ*M*(1,2,3)	119.62	119.96	121.9	121.82	122.48	122.02	121.10
M(4)	22.18	22.08	22.49	22.35	22.75	22.34	22.39
A	13.08	14.66	12.97	12.09	12.94	14.56	13.23
O(3)	17.24	16.8	17.37	17.51	17.26	17.28	17.29
Calculated (from the unit formulae in Table 5)							
Σ*M*(1,2,3)	120.67	120.77	121.26	121.55	122.86	121.16	119.22
M(4)	22.44	22.19	22.99	22.38	23.34	22.32	22.40
A	13.43	14.86	12.45	13.25	13.28	15.11	14.32

Standard deviations for refined site-scatterings are ≤0.05 *epfu*.

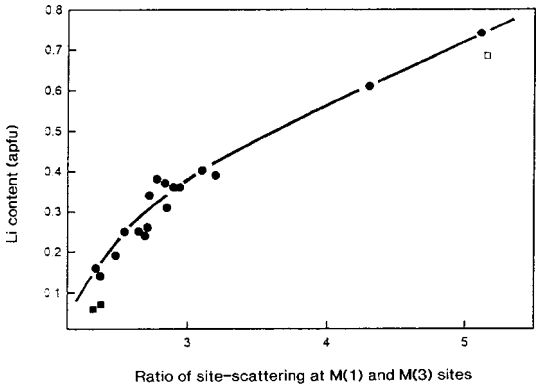

FIG. 2. Variation in Li content of alkali amphiboles (black circles) as a function of the ratio of the refined site-scattering values at the $M(1)$ and $M(3)$ sites [$S^{M(1)} / S^{M(3)}$]; data of this work and Hawthorne *et al.* (1993); black squares indicate sodic–calcic amphiboles, the hollow square indicates a Ti-rich amphibole.

for which this information is available (Fig. 2). There is a very well-defined relation, indicating that we can rapidly estimate the Li content in sodic amphiboles directly from the X-ray scattering at the $M(1)$ and $M(3)$ sites. There are three points that deviate somewhat from the monotonic relation of Figure 2. The amphiboles A(2) and A(7) (Fig. 2: black squares) from Hawthorne *et al.* (1993) are actually sodic–calcic amphiboles, rather than sodic amphiboles, and hence have a significantly different K_d value for the distribution of Fe^{2+} (and Mg) over $M(1)$ and $M(3)$, accounting for their deviation from the sodic-amphibole trend of Figure 2. Amphibole A(1) (Fig. 2: hollow square) of Hawthorne *et al.* (1994) is a titaniferous amphibole with 0.41 Ti *pfu* (per formula unit) at the $M(1)$ site; this Ti affects the relative scattering at $M(1)$ and $M(3)$ in this particular crystal, accounting for its deviation from the trend of Figure 2. Thus the ratio of the scattering at the $M(1)$ and $M(3)$ sites is a useful indicator of Li content in alkali amphiboles (from the empirical relation depicted in Fig. 2).

The behavior of Ti

Previous work on amphiboles has shown that Ti can occur at the $T(2)$ site (Oberti *et al.* 1992, Della Ventura *et al.* 1991, 1993, Mottana *et al.* 1990, Paris *et al.* 1993) and the $M(1)$ site (Kitamura *et al.* 1975, Pechar *et al.* 1989, Oberti *et al.* 1992); furthermore, many authors have proposed that the normally small amounts of Ti in most amphiboles occur at the $M(2)$ site, whereas incorporation at the $M(3)$ site may occur in Fe-free kaersutite (Tiepolo *et al.* 1999). In the present case, we have an ideal opportunity to examine the behavior of Ti because of the lack of Mg and $^{[6]}$Al in these crystals. With regard to X-ray scattering, Ti ($Z = 22$) scatters less than Fe ($Z = 26$); this difference, together with the variation of Ti in these crystals, should give rise to small but significant differences in site scattering among these crystals. Figure 3 shows the variation in the refined scattering at the $M(1)$ site as a function of the amount of Ti in the crystal; the line in Figure 3 shows the ideal variation in scattering for occupancy of $M(1)$ by Fe and Ti. The variation in Figure 3 is linear and correlated with the ideal variation for Fe $\rightleftharpoons$ Ti substitution at $M(1)$, providing strong evidence for the incorporation of Ti at $M(1)$ in these amphiboles. Moreover, there is no such relation involving Ti and the refined site-scattering values at the $M(2)$ site.

The equivalent isotropic-displacement factors at the $M(1)$ sites are larger than the corresponding values at the $M(2)$ and $M(3)$ sites. These high values are indicative of positional disorder of (Fe,Mg) and Ti at $M(1)$, the latter cation being shifted toward the O(3)–O(3)

TABLE 6. ELECTRON- AND ION-MICROPROBE DATA FOR STRANGE LAKE AMPHIBOLES

	SL(1)	SL(2)	SL(3)	SL(4)	SL(5)	SL(6)	SL(7)
SiO_2 wt%	50.41	50.06	50.37	50.29	49.53	50.74	50.91
TiO_2	1.76	0.47	0.94	0.63	1.11	0.87	0.81
Al_2O_3	0.25	0.15	0.38	0.43	0.41	0.14	0.17
FeO	21.69	20.54	22.54	23.38	24.06	21.24	20.44
Fe_2O_3	11.17	11.8	12.53	11.68	10.83	11.93	12.97
MnO	0.97	1.95	0.62	0.50	0.62	1.35	1.20
ZrO_2	0.53	0.07	0.13	0.07	0.14	0.51	0.10
ZnO	0.49	1.01	0.28	0.20	0.24	0.71	0.67
MgO	0.00	0.05	0.01	0.05	0.04	0.00	0.05
CaO	0.11	0.11	0.24	0.25	0.40	0.21	0.26
Na_2O	8.39	7.78	8.34	8.80	8.39	8.21	8.35
K_2O	1.78	2.65	1.45	1.37	1.40	2.42	2.1
Li_2O	0.63	0.62	0.59	0.54	0.46	0.59	0.55
F	1.87	1.63	2.02	2.38	2.06	1.77	1.95
H_2O	0.66	1.02	0.69	0.61	0.62	0.77	0.79
O=F	–0.79	–0.69	–0.85	–1.00	–0.87	–0.75	–0.82
Total	99.39	99.15	100.14	100.10	99.29	100.20	100.39
Si *apfu*	7.950	7.971	7.919	7.924	7.903	7.974	7.970
Al	0.046	0.028	0.070	0.076	0.081	0.026	0.030
ΣT	7.996	7.999	7.989	8.000	7.984	8.000	8.000
Al	0.000	0.000	0.000	0.004	0.000	0.000	0.001
Fe^{3+}	1.326	1.414	1.482	1.385	1.300	1.411	1.528
Ti	0.205	0.056	0.111	0.075	0.133	0.103	0.095
Zr	0.041	0.005	0.010	0.005	0.011	0.039	0.008
Zn	0.057	0.119	0.033	0.023	0.028	0.082	0.077
Mg	0.000	0.012	0.000	0.012	0.010	0.000	0.012
Li	0.400	0.397	0.373	0.342	0.295	0.373	0.346
Fe^{2+}	2.860	2.736	2.924	3.081	3.211	2.791	2.677
Mn^{2+}	0.111	0.262	0.038	0.067	0.032	0.180	0.159
$\Sigma M(1,2,3)$	5.004	5.001	5.011	4.994	5.016	4.979	4.903
Mn^{2+}	0.019	0.001	0.045	0.000	0.052	0.000	0.000
Ca	0.019	0.019	0.040	0.042	0.068	0.035	0.044
Na	1.962	1.980	1.913	1.958	1.880	1.965	1.956
$\Sigma M(4)$	2.000	2.000	2.000	2.000	2.000	2.000	2.000
Na	0.603	0.422	0.629	0.730	0.715	0.536	0.578
K	0.358	0.538	0.291	0.275	0.285	0.485	0.419
ΣA	0.961	0.960	0.920	1.005	1.000	1.021	0.997
OH	0.694	1.083	0.723	0.641	0.660	0.807	0.825
F	0.938	0.826	1.010	1.191	1.045	0.885	0.970
O	0.368	0.091	0.268	0.168	0.295	0.308	0.205
ΣX	2.000	2.000	2.000	2.000	2.000	2.000	2.000

* Determined by stoichiometry.

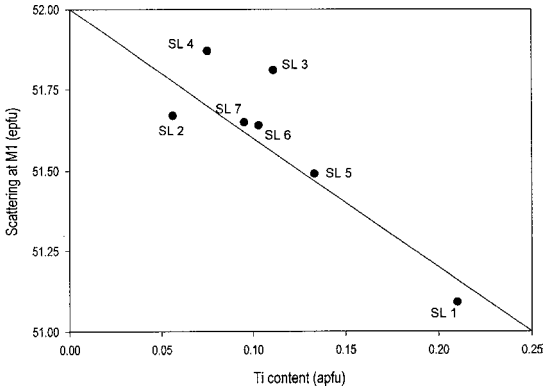

FIG. 3. Variation in the refined site-scattering at the *M*(1) site as a function of the amount of Ti in the structure as determined by electron-microprobe analysis. The line indicates the relation for 1:1 Fe ↔ Ti substitution.

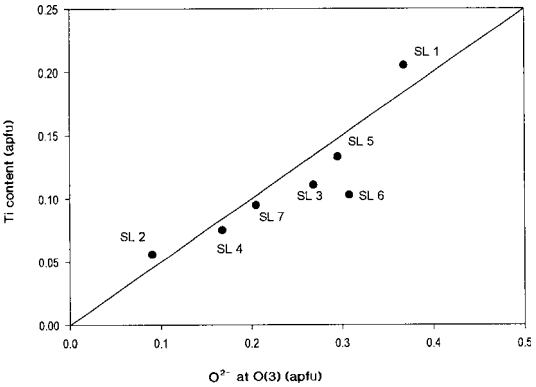

FIG. 4. Variation in Ti content as a function of O^{2-} content at the O(3) site for Strange Lake amphiboles; the line indicates the substitution Ti + 2 $^{O(3)}O^{2-}$ ⇌ (Mg,Fe^{2+}) + 2 $^{O(3)}(OH)^{-}$.

edge. This finding suggests that Ti is incorporated into these amphiboles *via* coupling with the local incorporation of O^{2-} at O(3) according to the relation $^{M(1)}$Ti + 2 $^{O(3)}O^{2-}$ ↔ $^{M(1)}$(Mg,Fe^{2+}) + 2 $^{O(3)}OH^{-}$. This relation indicates a 1 : 2 correlation between the Ti content and the amount of O^{2-} incorporated at O(3); Figure 4 shows this to be the case for the Strange Lake amphiboles.

The behavior of Mn

Site scattering by X-rays cannot distinguish between Fe^{2+} and Mn^{2+}. However, Mn^{2+} ($^{[6]}r$ = 0.83 Å) is larger than Fe^{2+} ($^{[6]}r$ = 0.78 Å), and hence mean bond-lengths can give an indication of the relative ordering of Fe^{2+} and Mn^{2+}. Inspection of Table 4 shows that <*M*(3)–O> is somewhat larger (~0.01–0.02 Å) than <*M*(1)–O> in these amphiboles, even where the Ti content is low. This difference suggests that Mn^{2+} is strongly ordered at the *M*(3) site, and site populations for Mn^{2+} were assigned accordingly.

The behavior of Zr

Crystals SL(1) and SL(2) have significant Zr present (~0.04 *apfu*), and we must consider the behavior of Zr in the amphibole structure. There are few data available concerning Zr in amphiboles. Pearce (1989) reported up to 0.33 Zr *apfu* in arfvedsonite from the Igaliko dyke swarm, south Greenland; the unit formulae exclude the possibility of Zr being a *B*-group cation, indicating that Zr is a *C*-group or a *T*-group cation. However, we suggest that the large difference in size between Zr ($^{[4]}r$ = 0.59 Å) and Si ($^{[4]}r$ = 0.26 Å) precludes the possibility of direct Zr ⇌ Si substitution. With regard to size ($^{[8]}r$ = 0.84, $^{[6]}r$ = 0.72 Å), Zr is expected to prefer the *C*-group sites over the *B*-group site. With regard to formal charge, Zr also is expected to be a *C*-group cation. Oberti *et al.* (2000a) compared the measured *M*–O interatomic distances with the elastic parameters calculated from the distribution coefficient between solid and liquid, $^{S/L}$D, for M^{4+} cations in synthetic Ti-rich amphiboles with Zr (and Hf) at the trace-element level, and deduced that Zr occurs at the *M*(2) site in pargasite and kaersutite from alkali basalts and basanites, and at the *M*(1) site in strongly dehydrogenated richterite from lamproite, the ruling criterion being the size of the relevant coordination polyhedra (i.e. cation of radius not larger than 2.080 Å).

The maximum Zr content in our crystals is ~0.04 *apfu* in SL(1) and SL(6); some information should be available from the refined site-scattering due to the high atomic number (40) of Zr. The behavior of crystal SL(6) in Figures 1 and 3 negates the possibility of Zr at the *M*(1) and *M*(3) sites; moreover, the refined scattering at the *M*(2) site in SL(6) is 52.46 *epfu* (Table 5), and its Zr content is 0.039 Zr *apfu*, corresponding to an increase of 0.55 *epfu* for that amount of Zr substituting for Fe. Thus there is direct indication that Zr is ordered at the *M*(2) site in these amphiboles.

The behavior of Zn

There is no way of objectively assigning site populations for Zn in these amphiboles; the scattering of Zn is only slightly different from that of Fe, and Zn is a divalent cation intermediate in size between Mg and Fe. The similarity in size and charge between Zn and (Mg, Fe^{2+}) suggests that Zn may not order at a specific site, but may be partly disordered over two or more *M* sites. Thus we include Zn with Fe^{2+} in the site populations of Table 7, and we express Fe^{2+} + Zn as Fe*.

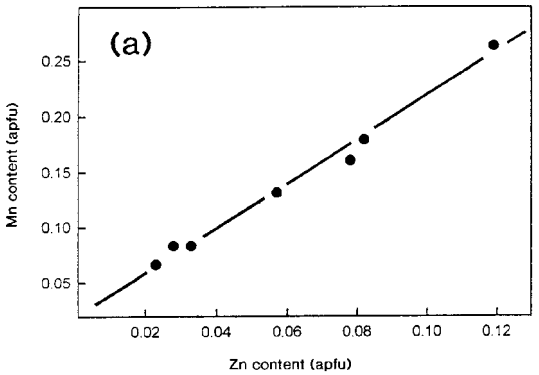

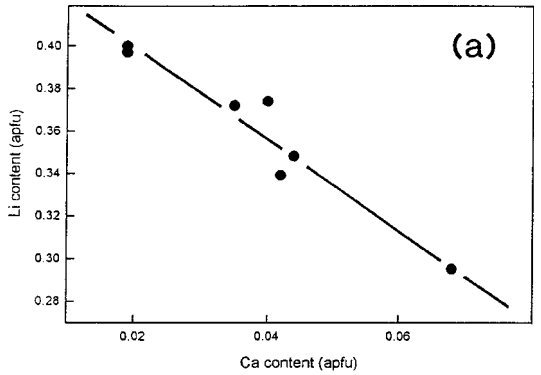

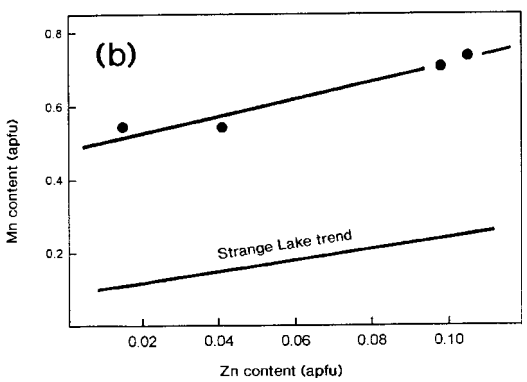

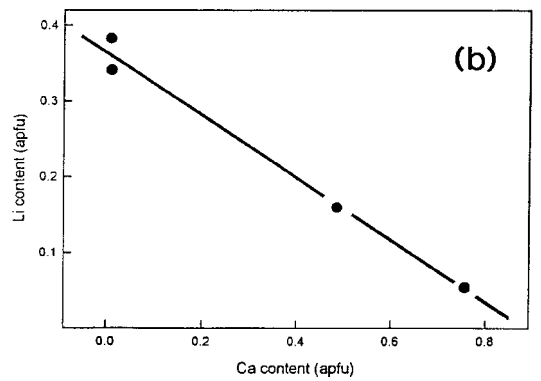

FIG. 5. Variation in the contents of Zn and Mn in cogenetic sodic–calcic and sodic amphiboles: (a) Strange Lake; (b) Virgin Canyon (Hawthorne *et al.* 1993); the lower line in (b) shows the Strange Lake trend.

FIG. 6. Variation in the contents of Li and Ca in cogenetic sodic–calcic and sodic amphiboles: (a) Strange Lake pluton; (b) Virgin Canyon pluton.

VARIATION IN COMPOSITION OF THE AMPHIBOLES

The Strange Lake amphiboles examined here show a very restricted range of composition. They are essentially Mg-free and very low in Ca and Al. They also show enrichment in unusual and incompatible elements such as Li, Zn, Zr and Mn. However, these unusual constituents differ in behavior among themselves. The Zn and Mn contents show a very strong positive correlation (Fig. 5a). Although both cations are expected to enter the *M*(1,2,3) sites [some electron density at the *M*(4") site would be present if Mn were a *B*-group cation: Oberti *et al*. (1993)], it is difficult to conceive of the correlation of Figure 5a being structurally induced by the amphibole. It seems more reasonable that this is an effect of progressive enrichment of both constituents in an evolving parent liquid. In this regard, we see a similar trend (Fig. 5b), but systematically enriched in Mn, in the amphiboles of the Virgin Canyon pluton, New Mexico (Hawthorne *et al.* 1993).

There is also a very strong correlation between the Li and Ca contents of the amphiboles from Strange Lake (Fig. 6a), decreasing level of Ca being accompanied by increasing level of Li. Thus far, octahedrally coordinated Li has been reported in large amounts (> 0.10 *apfu*) only in Fe-rich sodic amphiboles and in very Li- and Fe-rich amphiboles from the Pedriza Massif (Spain), which have mixed Li and Na occupancies (in nearly all proportions) at the *B*-group site (Caballero *et al*. 1998, Oberti *et al*. 2000b); Hawthorne *et al.* (1994) gave sound crystal-chemical reasons to constrain incorporation of Li in octahedral sites to these compositions. However, the trend of Figure 6a involves only very small amounts of Ca and moderate amounts of Li, and hence the mechanisms outlined by Hawthorne *et al.* (1994) cannot be invoked. The trend of Figure 6 must be an effect of progressive fractionation rather than a crystal-chemical effect of the amphibole structure itself. An analogous trend is also shown by the amphiboles from Virgin Canyon (Hawthorne *et al.* 1993). However,

TABLE 7. SITE-POPULATIONS (*apfu*)* FOR STRANGE LAKE AMPHIBOLES

		SL(1)	SL(2)	SL(3)	SL(4)	SL(5)	SL(6)	SL(7)
T(1)	Si	3.95	3.97	3.93	3.92	3.92	3.97	3.97
	Al	0.05	0.03	0.07	0.08	0.08	0.03	0.03
T(2)	Si	4	4	4	4	4	4	4
M(1)	Fe*	1.80	1.94	1.89	1.92	1.87	1.90	1.90
	Ti	0.20	0.06	0.11	0.08	0.13	0.10	0.10
M(2)	Fe*	0.59	0.56	0.52	0.62	0.75	0.72	0.64
	Fe^{3+}	1.37	1.43	1.47	1.38	1.24	1.24	1.35
	Zr	0.04	0.01	0.01	0.00	0.01	0.04	0.01
M(3)	Li	0.40	0.40	0.37	0.34	0.30	0.37	0.38
	Fe*	0.49	0.34	0.59	0.59	0.67	0.45	0.46
	Mn^{2+}	0.11	0.26	0.04	0.07	0.03	0.18	0.16
M(4)	Ca	0.02	0.02	0.04	0.04	0.07	0.04	0.04
	Na	1.96	1.98	1.92	1.96	1.88	1.96	1.96
	Mn^{2+}	0.02	0	0.04	0	0.05	0	0
A	Na	0.60	0.42	0.61	0.73	0.72	0.52	0.58
	K	0.36	0.54	0.29	0.27	0.28	0.48	0.42
O(3)	OH	0.67	1.06	0.76	0.65	0.69	0.91	0.83
	F	0.93	0.82	1.02	1.19	1.05	0.89	0.97
	O	0.40	0.12	0.22	0.16	0.26	0.20	0.20

* Fe* = Fe^{2+} + Zn

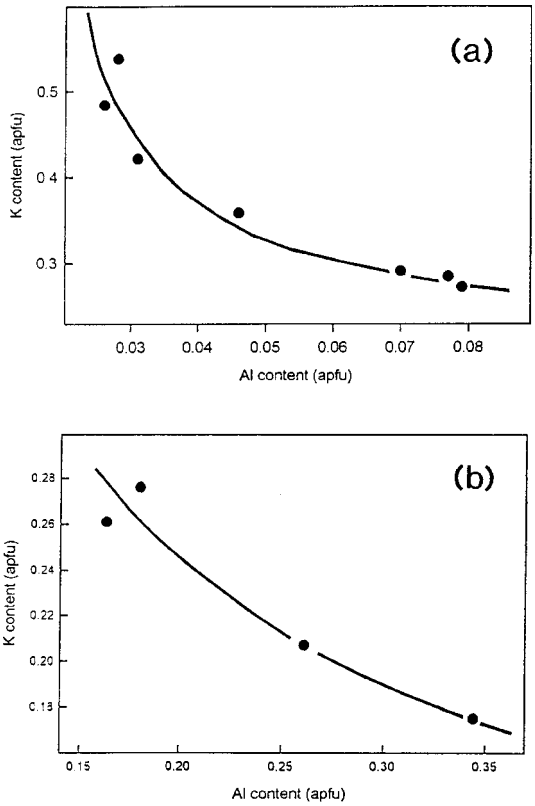

FIG. 7. Variation in the contents of K and Al in cogenetic sodic–calcic and sodic amphiboles: (a) Strange Lake; (b) Virgin Canyon.

the variation in composition at Virgin Canyon, specifically Ca, is greater than that shown by the Strange Lake amphiboles (Fig. 6b), and Ca–Li avoidance may be involved in the Strange Lake amphiboles. Although both these plutons are A-type granites, the low Ca content of the Strange Lake suite implies a greater degree of geochemical evolution of the parental granitic magma than at Virgin Canyon. However, as at Virgin Canyon, enrichment of Li during fractionation is coupled (in a crystal-chemical sense) to enrichment of Fe^{3+} in the magma. At Strange Lake, progressive increase in the intrinsic oxygen fugacity of the felsic magma is attributed to saturation in H_2O, bubble formation and degassing, leading to preferential loss of H and formation of hydrocarbons (Salvi & Williams-Jones 1997, Roelofsen 1997).

There is a well-developed relation between the K and Al contents of the Strange Lake amphiboles (Fig. 7). As the Al contents are so low (0.02–0.08 *apfu*), it is difficult to invoke a crystal-chemical mechanism. Moreover, the sequence [SL(4) SL(5) SL(3) SL(1) SL(7) SL(6) SL(2)] ordered according to increasing K corresponds to the sequence of samples with increasing Mn and Zn (Fig. 5a). This progressive build-up (and the relative depletion in Ca, Mg and Ti) reaches a maximum in sample SL(2). The *mafic* nature of the host rock for amphibole SL(2) is unusual: arfvedsonitic amphibole is its dominant constituent. The mafic clots are, in fact, a rare culmination of the agpaitic trend of crystallization, much more commonly developed in SiO_2-undersaturated rocks (*cf.* Khomyakov 1995). The amphibole-group mineral growing in this residuum is likely to depart significantly in composition from the ideal formula of arfvedsonite by incorporation of significant levels of incompatible elements. The approximate equivalence of arfvedsonitic amphibole and peralkaline mafic residuum makes this a possible example of indifferent states, a rare and poorly understood phenomenon in igneous petrogenesis (Nicholls 2000).

ACKNOWLEDGEMENTS

We thank John Schumacher, Nikita Chukanov and Associate Editor Ole Johnsen for their comments on this manuscript. This work was supported by Natural Sciences and Engineering Research Council of Canada grants to FCH and RMM and by Consiglio delle Ricerche (of Italy) funding to CSCC scientists.

REFERENCES

ARMBRUSTER, T., OBERHÄNSLI, R., BERMANEC, V. & DIXON, R. (1993): Hennomartinite and kornite, two new Mn^{3+} rich silicates from the Wessels mine, Kalahari, South Africa. *Schweiz. Mineral. Petrogr. Mitt.* **73**, 349-355.

BIRKETT, T.C., MILLER, R.R., ROBERTS, A.C. & MARIANO, A.N. (1992): Zirconium-bearing minerals of the Strange Lake intrusive complex, Quebec–Labrador. *Can. Mineral.* **30**, 191-205.

BOILY, M. & WILLIAMS-JONES, A.E. (1994): The role of magmatic and hydrothermal processes in the chemical evolution of the Strange Lake plutonic complex, Québec–Labrador. *Contrib. Mineral. Petrol.* **118**, 33-47.

CABALLERO, J.M., MONGE, A., LA IGLESIA, A. & TORNOS, F. (1998): Ferri-clinoholmquistite, $Li_2(Fe^{2+},Mg)_3Fe^{3+}{}_2Si_8O_{22}(OH)_2$, a new ^{B}Li clinoamphibole from the Pedriza Massif, Sierra de Guadarrama, Spanish Central System. *Am. Mineral.* **83**, 167-171.

DELLA VENTURA, G., ROBERT, J.-L. & BÉNY, J.-M. (1991): Tetrahedrally coordinated Ti^{4+} in synthetic Ti-rich potassic richterites: evidence from XRD, FTIR and Raman studies. *Am. Mineral.* **76**, 1134-1140.

_____, _____, _____, RAUDSEPP, M. & HAWTHORNE, F.C. (1993): The OH–F substitution in Ti-rich potassium-richterites: Rietveld structure refinement and FTIR and micro- Raman spectroscopic studies of synthetic amphiboles in the system K_2O–Na_2O–CaO–MgO–SiO_2–TiO_2–H_2O–HF. *Am. Mineral.* **78**, 980-987.

HAWTHORNE, F.C. (1978): The crystal chemistry of the amphiboles. VIII. The crystal structure and site-chemistry of fluor-riebeckite. *Can. Mineral.* **16**, 187-194.

_____ (1983): The crystal chemistry of the amphiboles. *Can. Mineral.* **21**, 173-480.

_____, OBERTI, R., OTTOLINI, L. & FOORD, E.E. (1996b): Lithium-bearing fluor-arfvedsonite from Hurricane Mountain, New Hampshire: a crystal-chemical study. *Can. Mineral.* **34**, 1015-1019.

_____, _____, UNGARETTI, L. & GRICE, J.D. (1992): Leakeite, $NaNa_2Mg_2(Fe^{3+}{}_2Li)Si_8O_{22}(OH)_2$, a new alkali amphibole from the Kajlidongri manganese mine, Jhabua district, Madhya Pradesh, India. *Am. Mineral.* **77**, 1112-1115.

_____, _____, _____, OTTOLINI, L., GRICE, J.D. & CZAMANSKE, G.K. (1996a): Fluor-ferro-leakeite, $NaNa_2(Fe^{2+}{}_2Fe^{3+}{}_2Li)Si_8O_{22}F_2$, a new alkali amphibole from the Cañada Pinabete pluton, Questa, New Mexico, U.S.A. *Am. Mineral.* **81**, 226-228.

_____, _____, ZANETTI, A. & CZAMANSKE, G.K. (1998): The role of Ti in hydrogen-deficient amphiboles. sodic–calcic and sodic amphiboles from Coyote Peak, California. *Can. Mineral.* **36**, 1253-1265.

_____, UNGARETTI, L., OBERTI, R., BOTTAZZI, P. & CZAMANSKE, G.K. (1993): Li: an important component in igneous alkali amphiboles. *Am. Mineral.* **78**, 733-745.

_____, _____, _____, CANNILLO, E. & SMELIK, E.A. (1994): The mechanism of $^{[6]}$Li incorporation in amphiboles. *Am. Mineral.* **79**, 443-451.

KAWAHARA, A. (1963): X-ray studies on some alkaline amphiboles. *Mineral. J.* **4**, 30-40.

KHOMYAKOV, A.P. (1995): *Mineralogy of Hyperagpaitic Alkaline Rocks*. Clarendon Press, Oxford, U.K.

KITAMURA, M., TOKONAMI, M. & MORIMOTO, N. (1975): Distribution of titanium atoms in oxy-kaersutite. *Contrib. Mineral. Petrol.* **51**, 167-172.

MILLER, R.R. (1996): Structural and textural evolution of the Strange Lake peralkaline rare-element (NYF) granitic pegmatite, Quebec–Labrador. *Can. Mineral.* **34**, 349-371.

MOTTANA, A., PARIS, E., DELLA VENTURA, G. & ROBERT, J.-L. (1990): Spectroscopic evidence for tetrahedrally-coordinated titanium in richteritic amphiboles. *Rend. Fis. Accad. Lincei* **9**, 387-392.

NICHOLLS, J. (2000): "Thermodynamics of a magmatic gas phase" 50 years later: comments on a paper by John Verhoogen (1949). *Can. Mineral.* **38**, 1313-1325.

OBERTI, R., CABALLERO, J.M., OTTOLINI, L., LÓPEZ-ANDRÉS, S. & HERREROS; V. (2000b): Sodic-ferripedrizite, a new monoclinic amphibole bridging the magnesium – iron – manganese – lithium and the sodium–calcium groups. *Am. Mineral.* **85**, 578-585.

_____, HAWTHORNE, F.C., UNGARETTI, L. & CANNILLO, E. (1993): The behaviour of Mn in amphiboles: Mn in richterite. *Eur. J. Mineral.* **5**, 43-51.

_____, UNGARETTI, L., CANNILLO, E. & HAWTHORNE, F.C. (1992): The behaviour of Ti in amphiboles. I. Four- and six-coordinate Ti in richterite. *Eur. J. Mineral.* **4**, 425-439.

_____, _____, _____, _____ & MEMMI, I. (1995): Temperature-dependent Al order–disorder in the tetrahedral double chain of *C*2/*m* amphiboles. *Eur. J. Mineral.* **7**, 1049-1063.

_____, VANNUCCI, R., ZANETTI, A., TIEPOLO, M. & BRUMM, R.C. (2000a): A crystal-chemical re-evaluation of amphibole/melt and amphibole/clinopyroxene D_{Ti} values in petrogenetic studies. *Am. Mineral.* **85**, 407-419.

OTTOLINI, L., BOTTAZZI, P. & VANNUCCI, R. (1993): Quantification of Li, Be and B in silicates by secondary ion mass spectrometry using conventional energy filtering. *Anal. Chem.* **65**, 1960-1968.

_____, _____, ZANETTI, A. & VANNUCCI, R. (1995): Determination of hydrogen in silicates by secondary ion mass spectrometry. *The Analyst* **120**, 1309-1313.

PARIS, E., MOTTANA, A., DELLA VENTURA, G. & ROBERT, J.-L. (1993): Titanium valence and coordination in synthetic richterite – Ti-richterite amphiboles: a synchrotron-radiation XAS study. *Eur. J. Mineral.* **5**, 455-464.

PEARCE, N.J.G. (1989): Zirconium-bearing amphiboles from the Igaliko dyke swarm, South Greenland. *Mineral. Mag.* **53**, 107-110.

PECHAR, F., FUESS, H. & JOSWIG, W. (1989): Refinement of the crystal structure of kaersutite (Vlčí Hora, Bohemia) from neutron diffraction. *Neues Jahrb. Mineral. Monatsh.*, 137-143.

ROELOFSEN, J.N. (1997): *The Primary and Secondary Mafic Silicates of two Alkaline Anorogenic Complexes: Strange Lake* (*Quebec–Labrador*) *and Amba Dongar* (*Gujarat, India*). Ph.D. thesis, McGill Univ., Montreal, Quebec.

SALVI, S. & WILLIAMS-JONES, A.E. (1997): Fluid-inclusion volatile analysis by gas chromatography: application of a wide-bore porous-polymer capillary column to the separation of organic and inorganic compounds. *Can. Mineral.* **35**, 1391-1414.

TIEPOLO, M., ZANETTI, A. & OBERTI, R. (1999): Detection, crystal-chemical mechanisms and petrological implications of $^{[6]}Ti^{4+}$ partitioning in pargasite and kaersutite. *Eur. J. Mineral.* **11**, 345-354.

Received June 12, 2000, revised manuscript accepted September 26, 2000.